

# Motor unit electrophysiological changes in Guillain-Barré syndrome in the context of a COVID-19 infection

A 55-year-old woman was admitted to the hospital with unstable gait followed by four-limb weakness with lower limb predominance. Several days before the onset of neurological symptoms, she developed mild respiratory symptoms, generalized myalgias without fever, and an episode of diarrhea.

On initial examination, she demonstrated moderate weakness mainly affecting the lower limbs (she could stand but was unable to walk), decreased proprioception, distal hypoesthesia, and generalized areflexia. A polymerase chain reaction nasal swab test was positive for severe acute respiratory syndrome–coronavirus 2; respiratory support was not required. Blood tests, cerebrospinal fluid analysis, chest X ray, and cranial computed tomography revealed no abnormalities.

Due to suspected Guillain-Barré syndrome (GBS), electrodiagnostic studies (EDx) were performed on day 9 after admission, and the patient was treated with intravenous immunoglobulin 0.4 g/kg for 5 days.

An initial nerve conduction study (NCS) revealed increased temporal dispersion (158%) and reduced proximal/distal compound muscle action potential (CMAP) size (0.5) in the right median and ulnar nerves with elbow stimulation (normal distal CMAP), reduced tibial

conduction velocities bilaterally (29 m/s), and absent tibial and median F waves. Thus, the patient met three criteria for demyelinating polyneuropathy.<sup>1</sup>

Electromyographic signals were recorded, using a 38 × 0.45-mm Neuroline concentric needle (Ambu, Ballerup, Denmark), from the right deltoid, extensor digitorum communis, first dorsal interosseous, tensor fascia latae, and vastus lateralis, and bilaterally from the tibialis anterior and gastrocnemius, and then bandpass filtered at 20 Hz to 10 kHz and stored using a KeyPoint.Net 3.22 device (Alpine Biomed, Fountain Valley, California). Spontaneous activity was qualitatively analyzed and motor unit potentials (MUPs) from electromyographic (EMG) signals with 200 ± 50 turns/s were quantitatively analyzed off-line using decomposition-based quantitative EMG<sup>2</sup> and near-fiber EMG (NFEMG),<sup>3,4</sup> which together aid in the diagnosis of neuromuscular disorders by quantifying intrinsic motor unit (MU) morphological and electrophysiological properties. A near-fiber MUP (NFM) is created by low-pass double-differentiation filtering a MUP, which, like SFEMG bandpass filtering, emphasizes contributions from fibers close to the needle detection surface (near fibers [NFs]). MUP area

## Left tibialis anterior

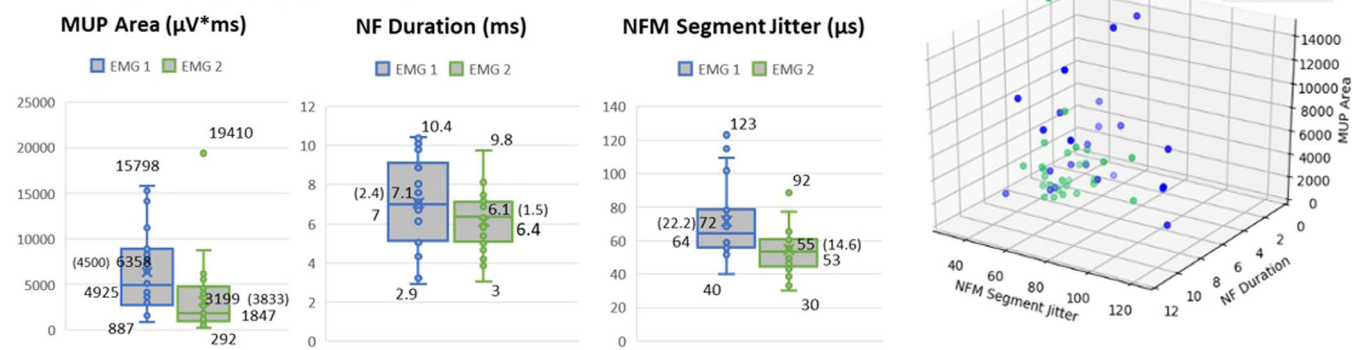


**FIGURE 1** Distribution of MUP and NFM values from the left tibialis anterior from two consecutive needle EMGs (n = 21 and 28, respectively). On the left, representative size, dispersion, and stability features are plotted (MUP area [ $\mu\text{V}\cdot\text{ms}$ ], NFM duration [ms], and NFM segment jitter [ $\mu\text{s}$ ], respectively). In each boxplot, minimum, maximum, median, and mean and standard deviation values are shown (mean values inside boxes and standard deviation in brackets). MUP area, NFM dispersion, and segment jitter were all reduced ( $P < .005$ , one-way analysis of variance test). On the right, a three-dimensional representation of all three measures for the pool of MUs sampled is shown. The MUP size and NFM temporal dispersion and instability for a majority of the MUs sampled during the first EMG examination (blue dots) are increased and more scattered compared with those of the MUs sampled during the second EMG examination (green dots). Abbreviations: EMG, electromyographic examination; MUP, motor unit potential; NF, near fiber; NFM, near-fiber MUP

**Abbreviations:** ANOVA, analysis of variance; CMAP, compound muscle action potential; COVID-19, coronavirus disease 2019; CSF, cerebrospinal fluid; EDx, electrodiagnostic study; EMG, needle electromyography; GBS, Guillain-Barré syndrome; L5, 5th lumbar

vertebra; MFAP, muscle fiber action potential; MU, motor unit; MUP, motor unit potential; NCS, nerve conduction studies; NF, near fiber; NFEMG, near-fiber electromyography; NFM, near-fiber motor unit potential; NMJ, neuromuscular junction.

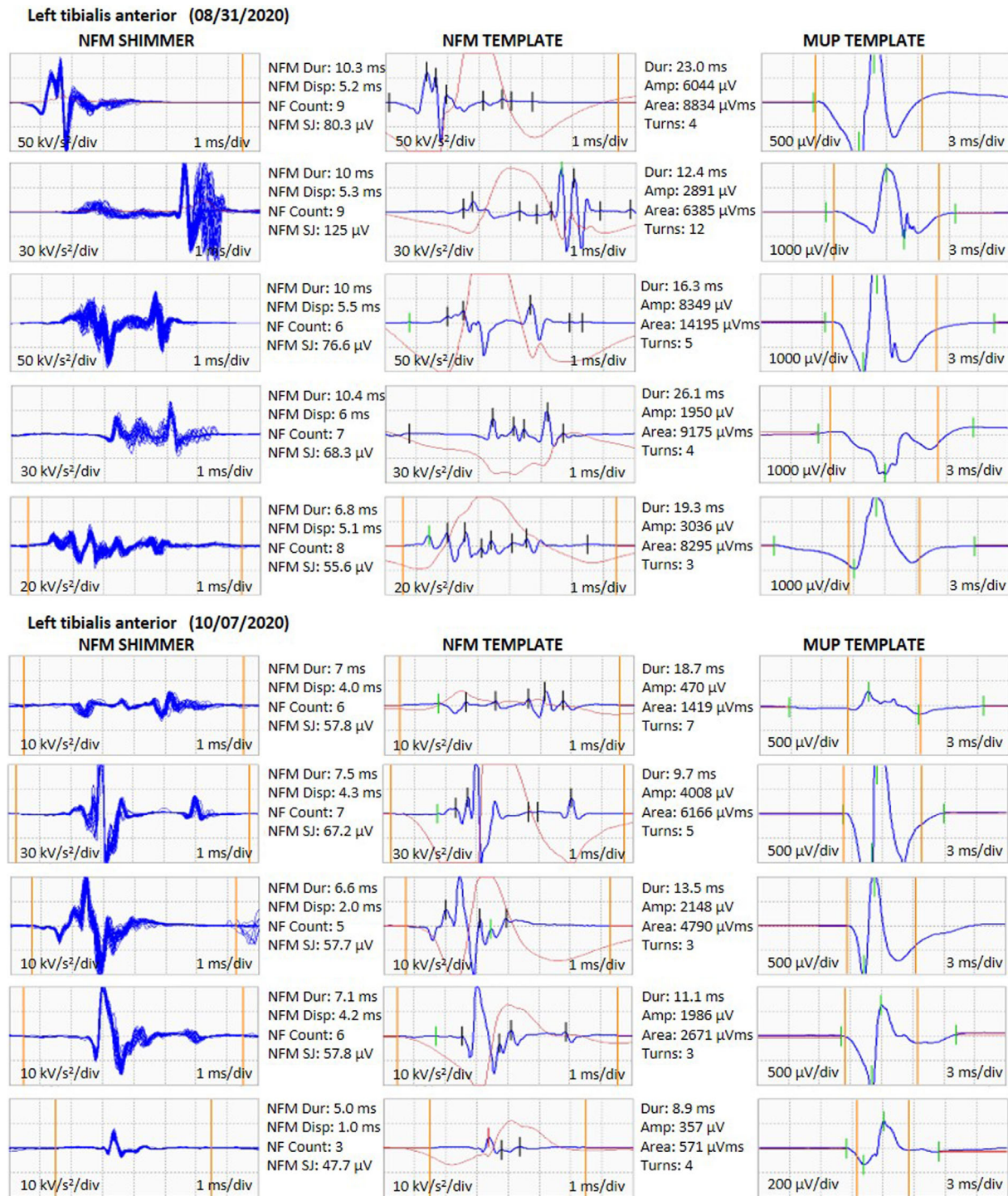


**FIGURE 2** Example MUPs/NFMs from the left tibialis anterior from two consecutive electromyographic examinations (upper and lower panel, respectively). MUPs shown were selected based on the representativeness of their values during each EMG. In the first examination, a majority of MUPs had increased size and NFMs had increased temporal dispersion and instability, compared with the second examination. From left to right: NFM shimmer, NFM template, and MUP template. The NFM shimmer shows overlapped isolated NFM traces. The top-to-bottom vertical lines indicate NFM duration. In the NFM template, each short vertical line corresponds to an NF peak. The time interval between the first and last short vertical line is the NFM dispersion. NFM and MUP feature values are shown: NFM duration (NFM Dur), NFM dispersion (NF Disp), near-fiber count (NF count), NFM segment jitter (NFM SJ), MUP duration (Dur), and MUP amplitude (amp) MUP area (area) number of MUP turns (turns). Abbreviations: EMG, electromyographic examination; MUP, motor unit potential; NF, near fiber; NFM, near-fiber MUP

represents MU size. NFM duration (the time between the NFM onset and end positions) and NFM dispersion (the time between the first and last detected NF contribution) do not reflect MU size; rather, they

reflect MU electrophysiological temporal dispersion (ie, differences in MU axonal branch conduction, neuromuscular junction [NMJ] transmission, and muscle fiber action potential [MFAP] conduction times).

NFM segment jitter reflects NFM temporal instabilities, caused by variability in MU axonal branch conduction, NMJ transmission, and MFAP conduction times.

Initially, low-amplitude and -frequency positive sharp waves and fibrillation potentials were recorded bilaterally from the tibialis anterior and gastrocnemius. Recruitment was reduced in all muscles sampled, with a predominance of large-area and irregularly shaped MUPs recorded from early-recruited MUs (more pronounced in distal lower limb muscles). Initial NFEMG measures showed increased dispersion and segment jitter in nearly all lower limb muscles sampled (Figure 1).

Subsequent EDx, performed 5 weeks later, showed improved NCS results. Although the criteria for demyelinating polyneuropathy were still met, significant clinical improvement was seen, as the patient was able to walk with minor assistance.

In addition, MUP area, NFM dispersion, and segment jitter were all reduced (Figure 1). Figure 2 shows examples of initial and subsequently recorded MUPs and NFM.

In GBS, early recruitment of MUs with large MUPs is a consequence of conduction block affecting small-diameter axons.<sup>5</sup> However, the electrophysiology of MUPs in GBS (ie, quantification of MUP size, temporal dispersion, and stability) is not usually included in the diagnostic protocols for GBS.<sup>6</sup> Our results could be explained by both a transient impairment of smaller diameter myelinated motor axons (possibly a consequence of conduction block affecting proximal nerve segments, manifesting as early recruitment of large MUs and reduced numbers of small area MUPs) and possible transient electrophysiological impairment of either MU distal axonal branches or their NMJs (manifesting as transient increased NFM dispersion and segment jitter).

Also, axonal degeneration and rapid regeneration of short myelinated segments of intramuscular terminal axonal branches has been associated with immune-mediated subtypes of GBS,<sup>7</sup> which could explain the early active denervation and rapid motor recovery observed.

These findings support the combined use of EMG and NFEMG in suspected polyneuropathy. Because MUP area reflects MU size while NFM duration, dispersion, and stability reflect MU electrophysiological dispersion and stability, respectively, their combined use can provide valuable information for early diagnosis and management of treatable disorders.

## KEYWORDS

electroneuromyography, Guillain-Barré syndrome, motor unit, neuromuscular transmission, polyradiculoneuropathy

## CONFLICT OF INTEREST

The authors declare no potential conflicts of interest.

## ETHICAL PUBLICATION STATEMENT

We confirm that we have read the Journal's position on issues involved in ethical publication and affirm that this report is consistent with those guidelines.

## DATA AVAILABILITY STATEMENT

Data available on request due to privacy/ethical restrictions

Oscar Garnés-Camarena MD<sup>1</sup>

Gonzalo Díaz-Cano MD<sup>1</sup>

Daniel Stashuk PhD<sup>2</sup>

<sup>1</sup>Department of Physical Medicine and Rehabilitation - Clinical Neurophysiology, Jiménez Díaz Foundation University Hospital, Madrid, Spain

<sup>2</sup>Department of Systems Design Engineering, University of Waterloo, Waterloo, Ontario, Canada

## Correspondence

Oscar Garnés-Camarena, Department of Physical Medicine and Rehabilitation - Clinical Neurophysiology, Jiménez Díaz, Foundation University Hospital, Av. Reyes Católicos 2 28040, Madrid, Spain.

Email: oscar.garnes@quironsalud.es

## REFERENCES

1. Uncini A, Kuwabara S. The electrodiagnosis of Guillain-Barré syndrome subtypes: where do we stand? *Clin Neurophysiol.* 2018;129:2586-2593.
2. Stashuk DW. Decomposition and quantitative analysis of clinical electromyographic signals. *Med Eng Phys.* 1999;21:389-404.
3. Piasecki M, Garnés-Camarena O, Stashuk D. Near-fibre electromyography. *Clin Neurophysiol.* 2021;132:1089-1104.
4. Estruch O, Cano G, Stashuk D. P32-S application of decomposition based quantitative EMG (DQEMG) to focal neuropathies. *Clin Neurophysiol.* 2019;130:e104.
5. Stalberg E, Trontelj J, Sanders D. *Single Fiber EMG.* 3rd ed. Fiskebäckskil: Edshagen; 2010.
6. Van Den Bergh P, Pieret F, Woodard JL, et al. Guillain-Barre syndrome subtype diagnosis: a prospective multicentric European study. *Muscle Nerve.* 2018;58:23-28.
7. Ho TW, Li CY, Cornblath DR, et al. Patterns of recovery in the Guillain-Barré syndromes. *Neurology.* 1997;48:695-700.